JOURNAL OF GEOPHYSICAL RESEARCH, VOL. 115, A06213, doi:10.1029/2009JA014847, 2010

Cassini observations of narrowband radio emissions in Saturn's magnetosphere

Z. Wang,[1] D. A. Gurnett,[1] G. Fischer,[1,2] S.-Y. Ye,[1] W. S. Kurth,[1] D. G. Mitchell,[3] J. S. Leisner,[1,4] and C. T. Russell[4]

Received 31 August 2009; revised 6 January 2010; accepted 26 January 2010; published 23 June 2010.

[1] The Radio and Plasma Wave Science instrument (RPWS) on board the Cassini spacecraft has detected numerous narrowband radio emissions in Saturn's magnetosphere from September 2005 to May 2007. Typically, the narrowband radio emissions occur after an intensification of Saturn kilometric radiation (SKR) and last for several days. These emissions often occur near 5 kHz, with a modulation period of about 10.8 h, similar to the planet's rotation period. Other apparently associated bands also occur at higher frequencies, typically from 20 to 30 kHz. Both 5 kHz and 20 to 30 kHz emissions tend to decrease in intensity with increasing time and slowly drift upward in frequency after the onset. Our study shows that the narrowband radio emissions tend to be observed on the nightside at a radial distance range from 5 to 50 Saturn radii and tend to be observed more frequently at higher latitudes. The rotational modulation of narrowband radio emissions in Saturn's magnetosphere acts like a flashing light rather than a rotating beacon, similar to the source of SKR. These emissions are believed to be generated by mode conversion from anisotropy-driven electrostatic instabilities near the upper hybrid frequency. Comparisons with Cassini neutral particle imaging data show that transient hot plasma clouds, corotating with the planet inside the orbit of Titan, might be the source for narrowband radio emissions. Comparisons with Cassini Magnetometer data reveal that the narrowband radio emissions tend to occur 1 or 2 days after the compression of the magnetotail.

Citation: Wang, Z., D. A. Gurnett, G. Fischer, S.-Y. Ye, W. S. Kurth, D. G. Mitchell, J. S. Leisner, and C. T. Russell (2010), Cassini observations of narrowband radio emissions in Saturn's magnetosphere, *J. Geophys. Res.*, *115*, A06213, doi:10.1029/2009JA014847.

1. Introduction

[2] Most of the radio emissions coming from planetary magnetospheres can be classified into two main categories based on their generation mechanisms. The first is cyclotron maser radiation, like the auroral kilometric radiation (AKR) from the Earth and the Saturn kilometric radiation (SKR) from Saturn, which are the most intense radiations detected in planetary magnetospheres (e.g., see review by *Zarka* [1998]). The second category consists of numerous weaker radio emissions with narrow bandwidths and lower frequencies, which are believed to be produced by mode conversion from electrostatic upper hybrid waves. These emissions were given different names, such as nonthermal continuum radiation, narrowband kilometric radiation (nKOM at Jupiter) [*Kaiser and Desch*, 1980], or myriametric radiation [*Jones*, 1983] by different researchers. There is still no unified name for these emissions, so in this paper we refer to them simply as narrowband radio emissions. The first observations of narrowband emissions were from Earth's magnetosphere by *Gurnett and Shaw* [1973]. They were further studied by *Gurnett* [1975], who described many of the characteristics of this radiation and introduced the name nonthermal continuum radiation as he noticed their smooth and continuous appearance in the time-frequency spectra. In fact, the emissions have numerous narrowband components, but the instrumentation used at the time did not have sufficient resolution to distinguish among them. Later it was recognized that the emissions have many narrowband components [*Kurth et al.*, 1981], so the term continuum radiation is usually no longer used. *Gurnett* [1975] also predicted a possible source region near the dawnside plasmapause, and suggested that the terrestrial continuum radiation is associated with electrostatic waves near the upper hybrid resonance frequency. Similar emissions are observed at Jupiter in the form of narrowband kilometric radiation (nKOM) as well as lower-frequency narrowband emissions [*Gurnett et al.*, 1983]. The first report of narrowband radio emissions at Saturn was given by *Gurnett et al.*

[1]Department of Physics and Astronomy, University of Iowa, Iowa City, Iowa, USA.
[2]Space Research Institute, Austrian Academy of Sciences, Graz, Austria.
[3]Johns Hopkins University Applied Physics Laboratory, Laurel, Maryland, USA.
[4]Institute of Geophysics and Planetary Physics, University of California, Los Angeles, California, USA.

0148-0227/10/2009JA014847

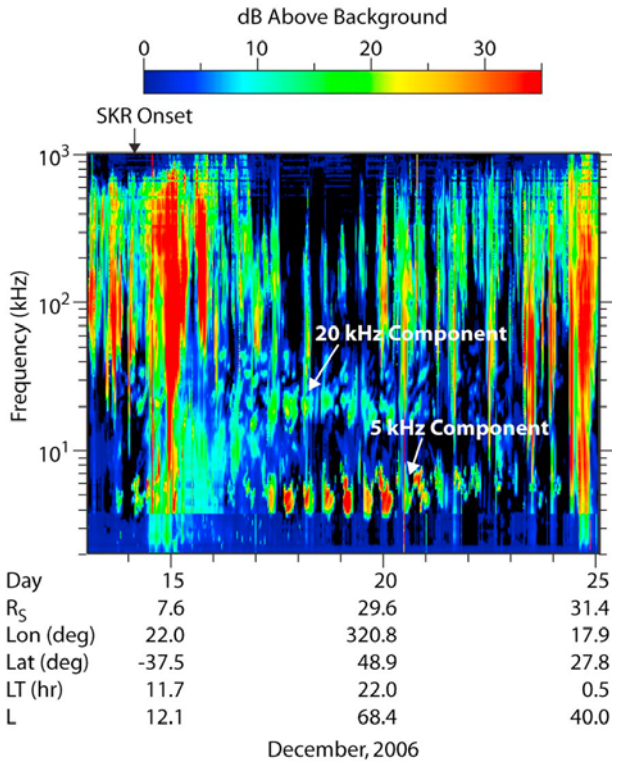

Figure 1. A typical Cassini RPWS spectrogram from 13 to 25 December 2006 showing several types of radio waves in Saturn's magnetosphere. The intense radio waves from 50 kHz to 500 kHz are Saturn kilometric radiation (SKR). The persistent periodic feature around 5 kHz is the narrowband radio emission. Near 20 kHz, there is another narrowband emission with much weaker intensity. Cassini trajectory data are given at the foot, specifically, the radial distance in Saturn radii, Voyager SLS longitude and latitude in degrees, local time (LT) in hours, and the L shell parameter.

[1981] after the Voyager 1 encounter with Saturn. The Voyager 1 Plasma Wave Science Instrument (PWS) detected the emissions over a range of radial distances from 3 to 58 R_s (Saturn radii). Since the plasma frequency is significantly below the wave frequency over much of this radial distance range, *Gurnett et al.* [1981] concluded that the radio emissions are freely propagating radio emissions generated by a source in the inner region of the magnetosphere.

[3] *Jones* [1988] first proposed that these narrowband radio emissions are produced by a linear mode conversion mechanism (LMC), and his theory is based on the assumption that electrostatic waves incident on a density gradient with the appropriate wave normal angle and near the plasma frequency would be converted into ordinary mode radio waves. A number of authors have also suggested a nonlinear conversion mechanism. Both linear conversion theory of *Jones* [1976, 1988] and nonlinear conversion mechanisms, described by *Melrose* [1981], *Barbosa* [1982], or *Rönnmark* [1983, 1989, 1992], have been proposed for the generation of Terrestrial Myriametric Radiation. *Rönnmark* [1989] estimated the efficiency of linear mode conversion and argued that it is three orders of magnitude too low to account for the observation. However, *Horne* [1989] showed in his ray tracing analysis that the path-integrated growth of electrostatic waves, which refract to the radio window, is more than sufficient to account for the observed Terrestrial Myriametric Radiation amplitudes. Some evidence has been found for each of the mechanisms, so they are not easily distinguishable for now. All of these mechanisms involve upper hybrid waves as the source. In the linear mechanism upper hybrid waves refract (in a steep density gradient) to Z mode waves first and the Z mode waves then mode convert to O mode waves at the radio window [*Horne*, 1989, 1990]. In the nonlinear mechanism, upper hybrid (UH) waves coalesce with some lower-frequency waves or scatter off of density irregularities to reach the free space mode. More recently, *Menietti et al.* [2009] suggested a possibility that Z mode waves can be directly generated by a loss cone distribution via the cyclotron maser instability. These Z mode waves later can mode convert to O mode in the presence of a density gradient.

[4] In this paper, we present observations, analysis and interpretations of the narrowband radio emissions observed at Saturn by the Cassini/RPWS instrument. In section 2 we describe the observations of the narrowband radio emissions and present our studies of their spectral and temporal characteristics. In section 3 we investigate their rotational modulation. In section 4 we briefly discuss a possible generation mechanism, based on the linear mode conversion theory including a possible source location model. Finally, in section 5 we discuss the correlation of the narrowband emissions with corotating plasma clouds injected after magnetotail compressions.

2. Observations

[5] Saturn narrowband radio emissions are recorded with bands A and B of the High Frequency Receiver (HFR) of the RPWS instrument [*Gurnett et al.*, 2004]. Band A, where the prominent 5 kHz component is recorded, covers the frequency range from 3.5 to 16 kHz, and band B goes from 16 to 71 kHz. Digital spectral analysis is performed within each of these bands to provide a choice of 8, 16, or 32 logarithmically spaced frequency channels with spectral resolutions of 20, 10, or 5%, respectively. The integration time can be either 0.125, 0.25, 0.5 or 1 s, and RPWS typically uses two or three antennas in band A and B which enables polarization and direction finding measurements [*Fischer et al.*, 2008; *Ye et al.*, 2009]. More details about RPWS on Cassini are given by *Gurnett et al.* [2004] and *Cecconi and Zarka* [2005].

[6] Figure 1 shows a typical Cassini RPWS wave spectrogram. This frequency-time spectrogram illustrates a variety of radio waves detected by RPWS in Saturn's magnetosphere. The frequency range in Figure 1 goes from 2 to 1000 kHz. The spectrum corresponds to nearly two weeks of observations, beginning on 13 Dec 2006 and ending on 25 December 2006. The intense radio waves at frequencies around 50 kHz and above are SKR. The periodic radio emissions with narrow banded features located at the bottom of the spectrogram are the narrowband radio emissions. The most intense and most frequently observed narrowband radio emissions are at frequencies of about 5 kHz. The bandwidth is 2 to 3 kHz, and one emission typically lasts for a few hours. Some apparently associated bands occur at higher frequencies, from 20 to 30 kHz. The intensities of the narrowband radio emissions clearly show a periodic modulation at about

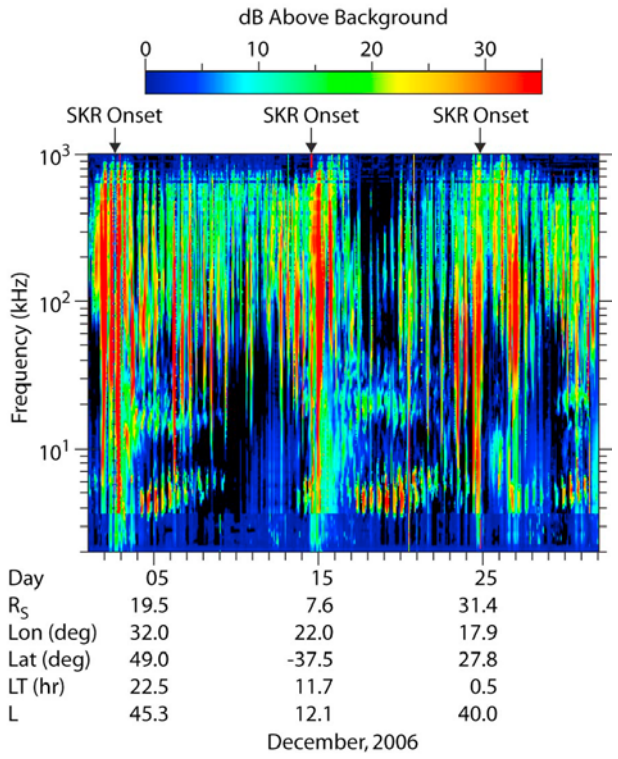

Figure 2. A spectrogram indicating the relationship between narrowband radio emissions and transient energetic SKR events in Saturn's magnetosphere. The narrowband emissions tend to occur after the onset of intense SKR, typically lasting several days with a slowly upward drifting frequency.

10.8 h (see section 3). These narrowband emissions can be detected over a large range of radial distance, and this observation provides the best evidence that the emissions consist of freely propagating electromagnetic waves. The intensity decreases gradually and the frequency slowly drifts upward with increasing time.

[7] *Louarn et al.* [2007] showed that the narrowband emissions typically occur after an energetic transient event in the magnetosphere that is indicated by an abrupt increase in the intensity of SKR. Figure 2 demonstrates this relationship between the narrowband radio emissions and the SKR. After the onset of the SKR burst, the narrowband emissions typically appear within 1 or 2 days and last for several days with a gradually decreasing intensity. In Figure 2 one can see three intensifications of SKR within one month around 2, 15, and 25 December. The intensifications are also normally accompanied by an extension of SKR down to lower frequencies, and each of these energetic events is followed by a series of about 10 rotationally modulated narrowband emissions lasting about 4 to 5 days. In the following we will call such a series of rotationally modulated emissions a narrowband emission event.

[8] Figure 3 shows a histogram of frequency drifts for narrowband radio emission events based on the data from September 2005 to May 2007. The horizontal axis is the drift rate and the vertical axis is the number of events. For every magnetospheric rotation, we record the frequency and time of the strongest emission point on the spectrogram. Then for each event, we obtained a series of frequency values. By doing a linear fit of these frequency values versus time, we computed the best fit of drift rate for every narrowband event. From the histogram we know that most of the events have an average drift rate of about 200–400 Hz per day. Possible reasons for this frequency drift are discussed in section 5.

[9] Due to the enhancement in sensitivity, and temporal and frequency resolution of the RPWS instrument compared to previous radio receivers, the fine structure of Saturn narrowband emissions can be resolved in unprecedented detail. Figure 4 illustrates the fine structure of narrowband radio emissions as it was recorded by the 10 kHz Wideband Receiver (WBR). The narrowband emissions have a finger-like shape, and the intensity is modulated with a period of about 15–25 min. Also, one can see a slight upward drift of this feature in frequency with increasing time. The reason why they have such fine structure is unclear and will be the subject of future study.

[10] The spatial distribution of the positions of Cassini during times when narrowband radio emissions are observed gives a general idea about the beaming of the narrowband emissions. In Figure 5, the gray lines show the trajectories of Cassini projected onto the equatorial plane and the meridian plane from September 2005 to May 2007. The black dots show the coverage of Cassini trajectories when narrowband emissions are observed. Figures 5 (top left) and 5 (top right) show the detection distribution of the 5 kHz component. It can be seen from Figure 5 (top left) that most 5 kHz components were detected in the evening sector. Although observable near the equator, the 5 kHz narrowband emissions are stronger and more easily detectable at higher latitudes. One likely reason that the emissions are more detectable at high latitude is because the dense plasma torus prevents the electromagnetic wave from propagating through to the equatorial area. This can in fact be clearly seen in the meridian plot in Figure 5 (top right). No 5 kHz emissions were detected close to the equatorial plane out to about 15 R_S, although the spacecraft

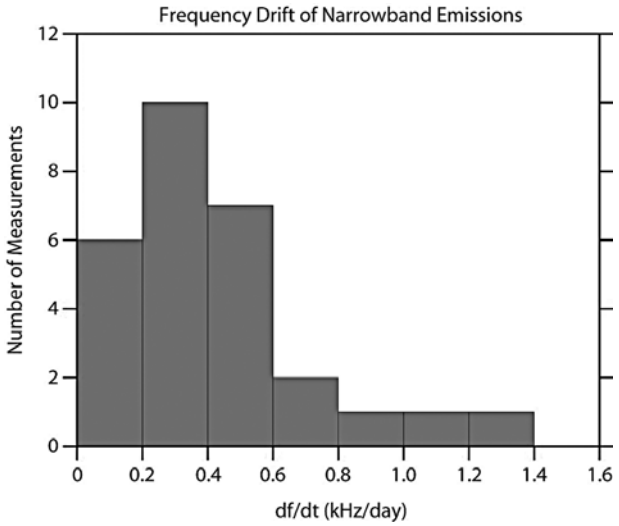

Figure 3. Histogram of drifting rates for narrowband radio emission events based on 2 years of data, from September 2005 to May 2007. The *x* axis is the drifting rate, and the *y* axis is the number of measurements.

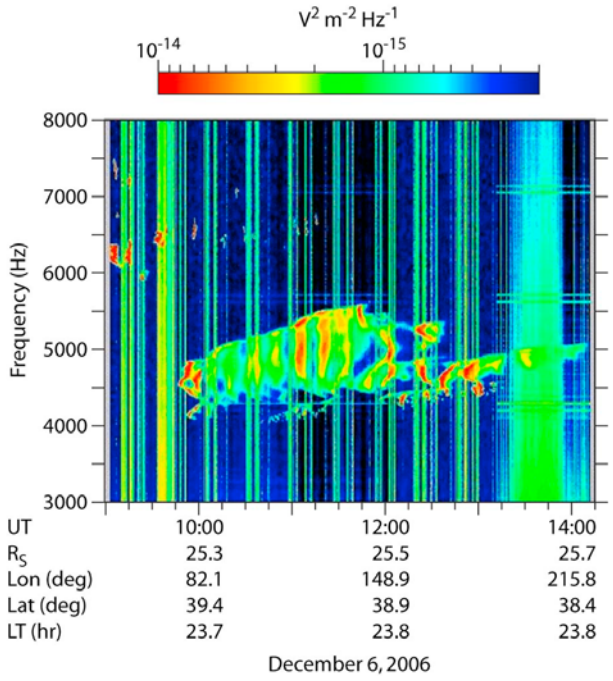

Figure 4. An example of narrowband radio emission fine structures observed by the WBR of Cassini/RPWS. The vertical stripes across the entire frequency range are due to changes in the receiver gain.

went through this region several times. Figures 5 (bottom left) and 5 (bottom right) show the detection distributions of the 20–30 kHz component. As can be seen, the occurrence of the 20–30 kHz narrowband emissions is generally confined to latitudes higher than 30 degrees (Figure 5, bottom right). There is one notable exception when Cassini is very close to Saturn (around 5 R_s). We believe that this is because the spacecraft crosses the source region in this case (see section 4). Figure 5 (bottom left) shows that the 20–30 kHz narrowband radio emissions are less frequently observed when Cassini is in the region of 0000–0003 LT and 1300–1500 LT. This is probably because from September 2005 to May 2007 Cassini went through the regions of ~0000 to 0003 LT and ~1300 to 1500 LT only at lower latitudes and detections of 20–30 kHz components are well confined to high latitudes. The extended regions over which Saturn narrowband emissions can be observed suggest that their beaming must be relatively broad and/or their sources are relatively extended. Table 1 is a list of 30 narrowband emission events where the latitudinal and local time ranges of the spacecraft during observations are given. There are 6 events (14, 15, 19, 23, 26, 28) where the local time changed by more than 7 h and the latitude by more than 60°. Despite those changes, there are no interruptions in the series of narrowband emissions that make up those events, which support the conclusion above.

[11] A more quantitative way to examine the occurrence probability of narrowband emissions is presented in Figure 6. In this plot, the magnetosphere is divided into small bins (local time versus latitude) and, for each bin, the ratio between the time of observation of the narrowband emissions and the total time that Cassini spent in the corresponding region is calculated. The color bar represents the occurrence probability of narrowband radio emission from 0 to 1. The white region is where the spacecraft did not fly through. As can be seen from Figure 6, Cassini was located in the Southern Hemisphere mostly on the dayside and in the Northern Hemisphere mostly on the nightside. The 5 kHz narrowband component (Figure 6, left) is more frequently observed in the evening sector (1800–2400), and the occurrence rate can be as high as 90%. The 5 kHz component is also more observable at higher latitude (>30 degrees) with an occurrence rate higher than 40%. One exception is in the region from 2200 to 0200 LT, where the narrowband radio emissions have a moderately high occurrence rate even at low latitudes. Compared to the 5 kHz component, the occurrence probability of the 20–30 kHz component is in general lower and confined to high latitudes (>40 degrees).

3. Rotational Modulation

[12] In this section we discuss the rotational modulation of narrowband radio emissions. The rotational modulation of magnetospheric radio emissions implies vital physical information and it reveals how the emissions are controlled by or correlated with other magnetospheric phenomena. For instance, *Warwick et al.* [1981] first showed that the rotational modulation of SKR acts more like a flashing light than a rotating beacon and *Gurnett et al.* [2007] proposed that this is linked to the rotational modulation of plasma and magnetic fields in the inner region of Saturn's plasma disk, near the moon Enceladus. *Zarka et al.* [2007] studied the fluctuation of the SKR period and reported a fluctuation by 1% with a timescale of 20–30 days and these fluctuations are correlated with solar wind speed at Saturn, which indicates that the SKR radio clock is controlled, at least partly by the conditions external to the planet's magnetosphere.

[13] We compare in Figure 7 the distribution of the intensity of the narrowband radio emissions over the longitude system of the Sun and the spacecraft, using the time-variable SKR longitude system SLS3 introduced by *Kurth et al.* [2008]. This SKR longitude system is based on a variable SKR period, which typically changes by a few seconds per month. It was introduced to get a more useful organization of magnetospheric phenomena. Figure 7 (left) is based on the SKR longitude of the Sun, and Figure 7 (right) is based on the SKR longitude of the spacecraft. In total, 9 events (18, 19, 20, 22, 23, 24, 25, 26, and 28) with large local time coverage are shown, from December 2006 to April 2007. It is essential to choose events with large local time coverage in order to confirm that the longitude is the controlling variable. In Figure 7, each colored stripe plots the integrated intensity (integrated over 10 min from 3.2 to 6.4 kHz) of one narrowband emission event (series of several hour-long emissions) as a function of longitude starting at the upper left corner, where the start time at zero longitude is indicated. We can see that, within one event, the narrowband radio emissions are organized much better in the system based on SKR longitude of the Sun. For example, for the emissions starting on day 360, 2006, with 9 h local time coverage, in Figure 7 (right) there is a clear drift over the longitude of the spacecraft. This result indicates that the modulation of narrowband emissions is like a flashing light and not like a rotating beacon. Hence, the narrowband radio emissions act like the SKR, which means that they tend to be "triggered"

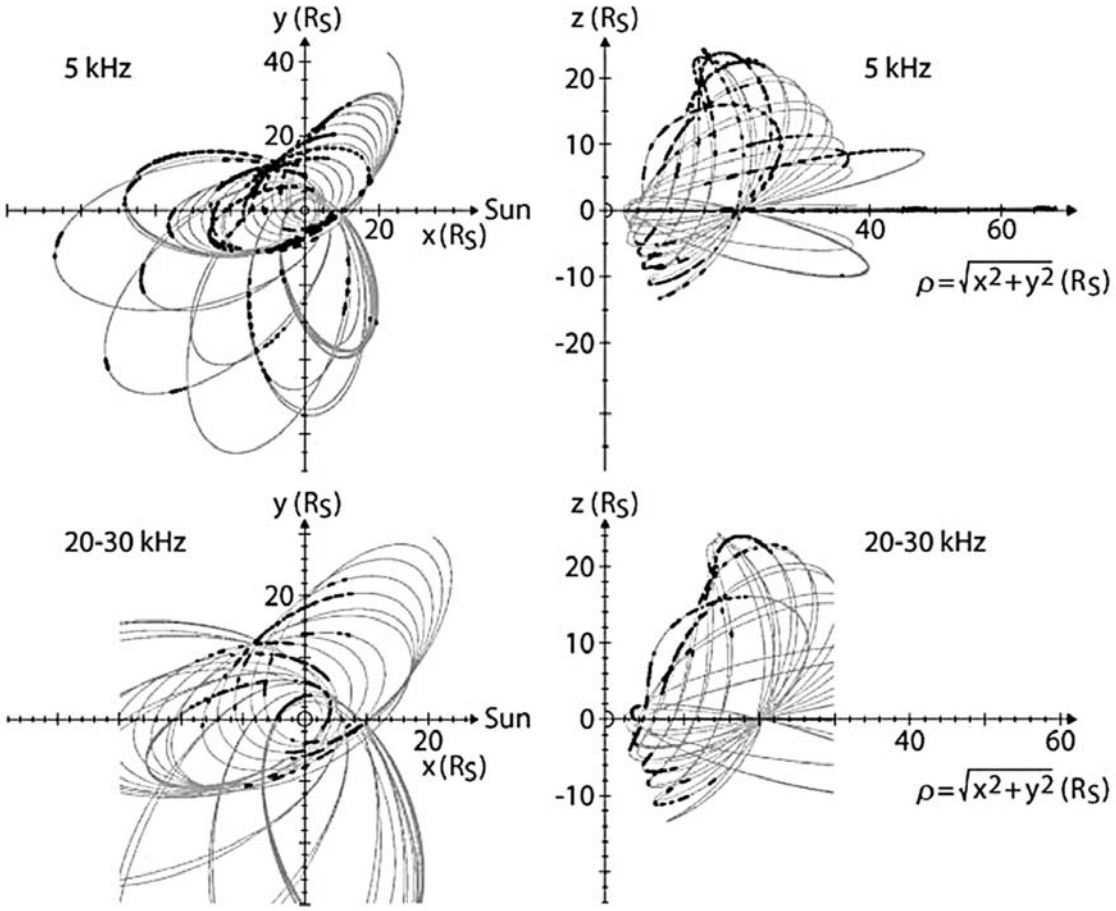

Figure 5. The gray lines show the trajectories of the Cassini spacecraft projected (left) onto the equatorial plane and (right) onto the meridian plane. The black dots show the positions of Cassini when it detected narrowband radio emissions projected onto the equatorial plane (Figures 5 (top left) and 5 (bottom left)) and onto the meridian plane (Figures 5 (top right) and 5 (bottom right)). The *X* axis is in the equatorial plane and in the plane containing the Sun and Saturn's spin axis, *Z* is along the spin axis, and *Y* completes the right-handed coordinate system. For the meridian plots, *Z* is along the spin axis, and ρ is the distance away from the planet projected on the equatorial plane. Figures 5 (top left) and 5 (top right) show the occurrence distributions for the 5 kHz emissions with a threshold of 10^{-14} W/m^2. Figures 5 (bottom left) and 5 (bottom right) show the occurrence distributions for 20–30 kHz emissions with the same threshold.

when Saturn achieves a given rotation orientation with respect to the Sun. Also, we notice that the SKR longitude of the Sun organizes all 9 events better as well compared to the SKR longitude of the spacecraft. It can be seen that the SKR longitude of the Sun was nearly 270° for the first event, and went to around 90° for the last one, dropping down 180° within 4 months. This drift indicates that the source for narrowband emissions is not completely rotating in synchronism with, but slightly faster (superrotate) than the SKR longitude system. For 12 December 2006 the rotation rate of the SLS3 system is ~798.3 deg/day (~10.82 h rotation period), and it changes slightly to 797.8 deg/day (~10.83 h) for 2 April 2007 [*Kurth et al.*, 2008]. The narrowband radio emissions exhibit a superrotation with respect to the SLS3 system of 1.23 ± 0.25 deg/day from December 2006 until April 2007, so their rotation period is ~10.81 h in this time interval. From Figure 5 of *Kurth et al.* [2008] one can see that the spreading of points around the interpolated line for the SLS3 period is around ± 2 deg/day or ± 0.03 h, which can be interpreted as the error for the determination of the rotation period for SKR as well as narrowband emissions. Figure 8 shows the narrowband radio emissions are well organized (with no drift in longitude) if SKR longitude system of the Sun is adjusted by applying the drift rate to the original one.

4. Generation Mechanism

[14] It is widely believed that, at Earth and Jupiter, narrowband radio emissions are generated by mode conversion from electrostatic upper hybrid resonance emissions in regions of large plasma density gradients associated with boundaries of the plasma sheet. When the matching condition, $f_{UH} \approx (n+1/2)\, f_c$, is satisfied, the electrostatic waves are most intense [*Gurnett et al.*, 1981]. In this matching condition f_{UH} is the upper hybrid frequency, f_c is the electron cyclotron frequency, and n = 1, 2, 3… is an integer. *Ye et al.* [2009]

Table 1. Narrowband Radio Emission Events From September 2005 Until May 2007

Event	Start Time	Stop Time	Latitude Range	LT Range	Plasma Cloud (Yes)	Simultaneous Onset
1	25 Sep 2005 (268)	29 Sep 2005 (272)	−0.2	4.2–6.3	yes	
2	24 Oct 2005 (297)	28 Oct 2005 (301)	−0.4	7.9–8.6	yes	
3	29 Nov 2005 (333)	7 Dec 2005 (341)	0.2– (−0.1)	3.6–5.5	yes	
4	5 Apr 2006 (095)	9 Apr 2006 (099)	0.2	2.2–2.8	?	
5	17 Apr 2006 (107)	20 Apr 2006 (110)	0.1	3.5–3.8	yes	
6	7 May 2006 (127)	11 May 2006 (131)	0.2	1.2–1.8	no data	
7	23 May 2006 (143)	29 May 2006 (149)	0.3–0.4	21–22.8	yes	
8	5 Jun 2006 (156)	11 Jun 2006 (162)	0.4–0.3	0.4–0.7	no data	
9	7 Jul 2006 (188)	15 Jul 2006 (196)	0.5	23.0–0	no data	
10	25 Jul 2006 (206)	2 Aug 2006 (214)	0–14.0	19.8–23.0	no data	
11	22 Aug 2006 (234)	27 Aug 2006 (239)	13.0–10.0	22.3–23.1	no data	
12	13 Sep 2006 (256)	20 Sep 2006 (263)	18.8–10.0	0.1–0.9	no data	
13	12 Oct 2006 (285)	15 Oct 2006 (288)	0–46.0	18–22	yes	yes
14	8 Nov 2006 (312)	13 Nov 2006 (317)	−30.0–40.0	13–23	312–315	
15	21 Nov 2006 (325)	24 Nov 2006 (328)	−17.0–40.0	14–23	yes	
16	26 Nov 2006 (330)	1 Dec 2006 (335)	0–2.0	0.8–2.5	no data	
17	4 Dec 2006 (338)	9 Dec 2006 (342)	0–50.0	20.2–0.9	338	yes
18	16 Dec 2006 (350)	23 Dec 2006 (358)	50.0–38.0	18–23.2	351, 352	
19	26 Dec 2006 (360)	1 Jan 2007 (365)	15– (−50.0)	1.0–10	yes	
20	8 Jan 2007 (008)	14 Jan 2007 (014)	40– (−12.0)	23.5–1.5	yes	
21	15 Jan 2007 (015)	18 Jan 2007 (018)	−12.0–30.0	2.5–8	yes	yes
22	19 Jan 2007 (019)	25 Jan 2007 (025)	30.0–55.0	16.4–22.3	yes	
23	3 Feb 2007 (034)	12 Feb 2007 (043)	−28.0–60.0	13.8–21.3	yes	
24	14 Feb 2007 (045)	21 Feb 2007 (052)	20.0– (−26)	2–6.2	yes	
25	27 Feb 2007 (060)	5 Mar 2007 (064)	60.0–22.0	20–0.8	60	
26	15 Mar 2007 (074)	22 Mar 2007 (081)	55.0– (−18)	16.5–24	yes	yes
27	23 Mar 2007 (082)	25 Mar 2007 (084)	−18.0– (−22)	6.2–11	yes	yes
28	2 Apr 2007 (092)	10 Apr 2007 (100)	50.0– (−20)	17.0–7.8	91–96, 99–100	
29	9 May 2007 (129)	12 May 2007 (132)	40.0– (−11)	19.7–21.8	yes	
30	22 May 2007 (142)	26 May 2007 (146)	20.0–28.0	16.3–19	yes	

show examples of RPWS detections of 20–30 kHz narrowband source regions, which is indicated as intense upper hybrid resonance followed by a series of narrowband radio emissions near 20–30 kHz. Up to now, RPWS has not detected any source crossings for 5 kHz narrowband emissions, possibly because the spacecraft rarely flies through the predicted 5 kHz source region. The generation mechanism of these electrostatic waves has not been fully understood. Among various types of electrostatic instabilities that can occur in a hot magnetized plasma, two broad classes of instabilities can be identified. One is the anisotropy-driven instability and the other is the current-driven instability. The electrostatic waves converting to narrowband radio emissions at Saturn belong to the former class [*Gurnett and Bhattacharjee*, 2005]. Previous studies showed that the generation of the electrostatic waves requires an electron plasma containing two components: a cold component (density n_C, temperature T_C) and a hot component with a positive slope in the perpendicular velocity distribution (density n_H, temperature T_H). A reasonable cold-to-hot electron density ratio n_C/n_H is also a necessary condition and it should not be too large (the cutoff is ~3–5). The cold electron density controls which frequency band is exited and the hot electrons with an anisotropy distribution provide the source of free energy to make the instability occur [*Rönnmark et al.*, 1978; *Hubbard and Birmingham*, 1978; *Ashour-Abdalla and*

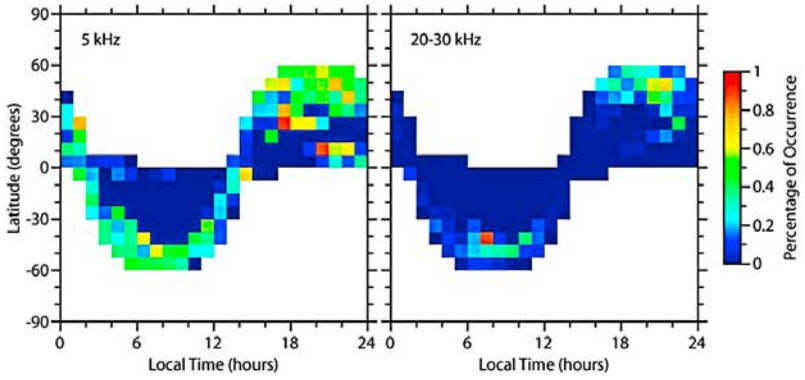

Figure 6. Occurrence rate of narrowband radio emissions in local time versus latitude space. The bin size is 1 h × 7.5 degrees. The color bar goes from 0 to 1, indicating the percentage of occurrence from 0 to 100%. (left) The occurrence rate of the 5 kHz emissions and (right) the occurrence rate of the 20–30 kHz emissions.

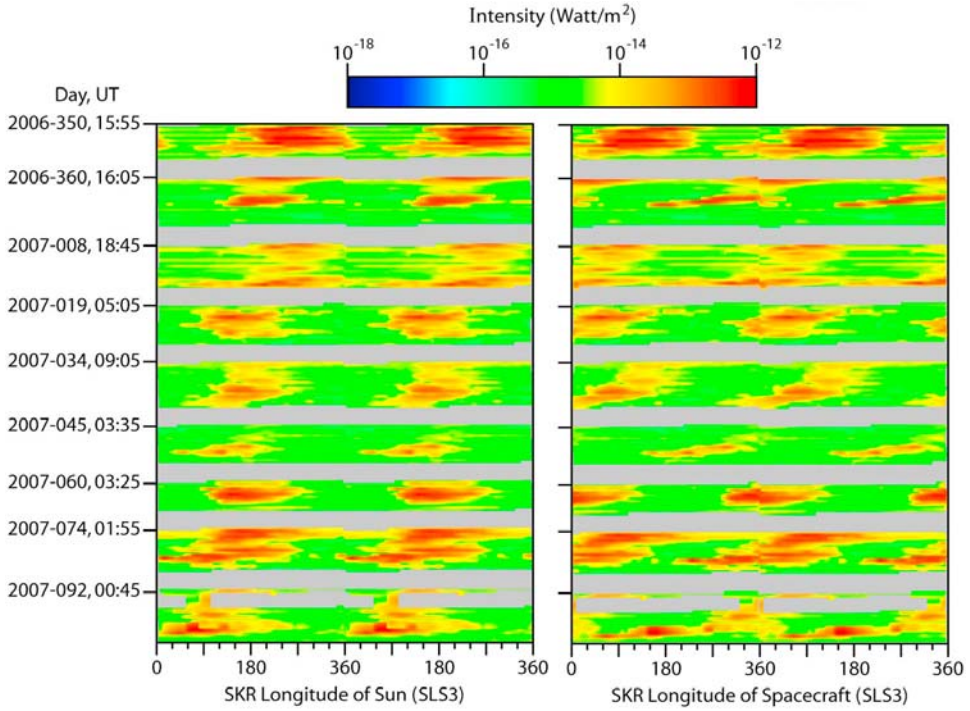

Figure 7. The distributions of 5 kHz narrowband radio emissions using two longitude systems. (left) Based on the SKR SLS3 longitude of the Sun and (right) based on the SKR SLS3 longitude of the spacecraft. For clarity, we have plotted it over two rotations.

Kennel, 1978]. Recently, polarization studies by *Fischer et al.* [2008] and *Lamy et al.* [2008] have shown that the 5 kHz narrowband components are ordinary mode emissions, since they are left-hand polarized when observed from the Northern Hemisphere and right-handed polarized when observed from the Southern Hemisphere (oppositely polarized to SKR). *Farrell et al.* [2005] have shown that some of the narrowband radio emissions observed by Cassini/RPWS interior to Saturn's plasma torus at radial distances less than 2.5 R_s are propagating in the Z mode. *Menietti et al.* [2009] postulate that in the presence of density gradients, Z mode emission can mode-convert into O mode emission, and this might explain the narrowband emission observed by the Cassini spacecraft.

[15] A possible model for the source positions of narrowband radio emissions in Saturn's magnetosphere is shown in Figure 9. The plasma density contour is derived from Persoon's electron density model [*Persoon et al.*, 2006]. The source is located at the northern and southern boundaries of the plasma sheet because in such a region, the existing plasma gradient can easily satisfy the matching condition, thus, the generation of narrowband radio emissions. As an example, we show for n = 1, the 5 kHz component source in the model, which is located near the intersection of the constant B contour with a cyclotron frequency of (3/2) f_c = 5 kHz, and the f_p = 5 kHz plasma frequency contour (indicated by the red dotted line, for n = 1 we have (3/2) $f_c = 3\ f_p/\mathrm{sqrt}(5) \approx f_p$). The L shell of this intersection is at about L = 7.4. For n greater than 1, the source location moves outward along the boundary of the plasma sheet. For the narrowband radio emissions with high frequencies, like those with 20 to 30 kHz, the source locations would be closer to the planet since as the frequency

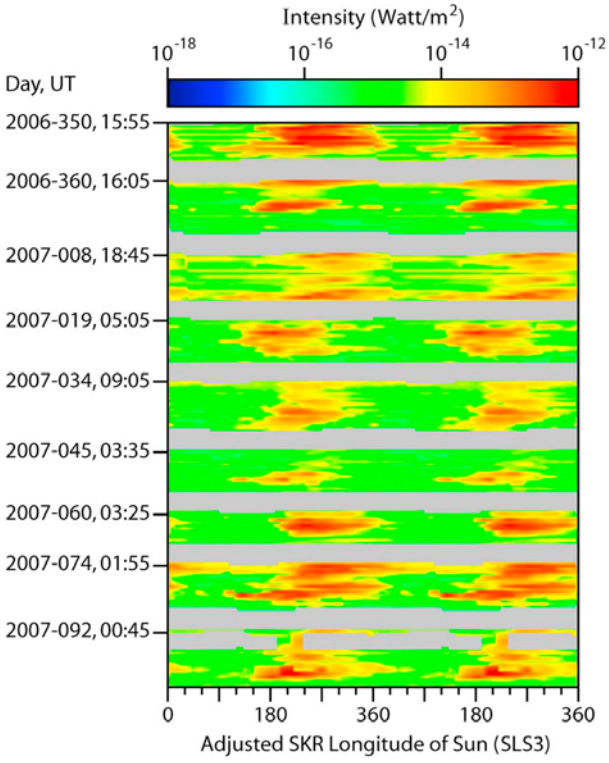

Figure 8. An upgraded version of Figure 7 (left), showing the 5 kHz narrowband radio emissions are well organized in this adjusted SKR longitude system by considering the drift rate.

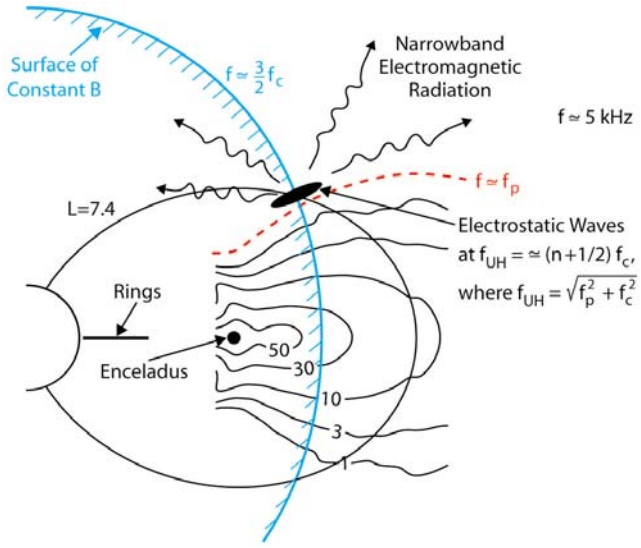

Figure 9. A model for generating narrowband radio emissions in Saturn's magnetosphere. These emissions are believed to be generated by mode conversion from electrostatic upper hybrid waves near the northern and southern boundaries of the plasma disk. The source of the 5 kHz emissions is located near the intersection of the constant B contour corresponding to a cyclotron frequency of (3/2) f_c = 5 kHz and the f_p = 5 kHz plasma frequency contour. This intersection occurs at L = 7.4.

increases, the constant B contours move closer to Saturn [*Ye et al.*, 2009].

5. Correlation of Narrowband Radio Emissions With Transient Hot Plasma Clouds and Magnetic Field Compressions in the Magnetotail

[16] In section 4 we briefly described the generation mechanism by which electrostatic upper hybrid waves are converted to the narrowband L-O mode emissions. We now know that for generating these electrostatic emissions, we must have a plasma which has a cold electron component and a hot electron component with a gentle loss cone distribution, and a reasonable density ratio between them. Using the Energetic Neutral Atom (ENA) technique the Magnetospheric Imaging Instrument (MIMI) Ion and Neutral Camera (INCA) on the Cassini spacecraft repeatedly observes transient rotating hot plasma clouds in the inner magnetosphere. The ENA technique relies on charge exchange between trapped ions and a cold neutral gas that results in fast neutral atoms escaping from the charge exchange region and being sensed as if they were photons [*Krimigis et al.*, 2007]. Plasma clouds observed by INCA imply a population of energetic ions that charge exchange with the neutrals. *Menietti et al.* [2009] have shown that the injected plasma clouds have a hot electron component with a loss cone distribution, thereby providing a free energy source that could drive electrostatic upper hybrid waves.

[17] Table 1 is a list of all the narrowband radio emission events detected by Cassini at Saturn, from September 2005 to

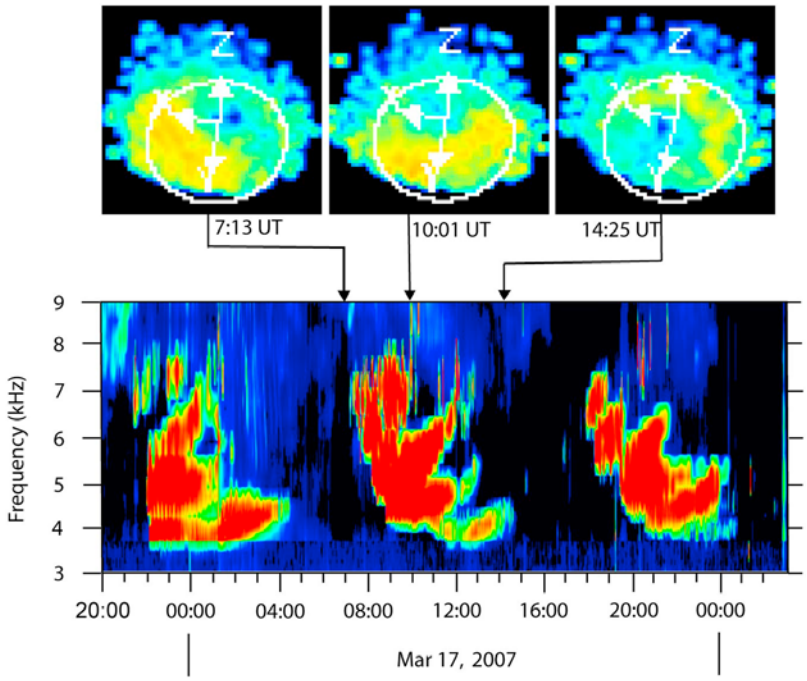

Figure 10. Comparison of ENA images from MIMI/INCA with an RPWS spectrogram of 17 March 2007. At the top, three ENA images which indicate that a hot plasma cloud was rotating around the planet and moving through the premidnight, midnight and postmidnight areas (Sun is on the left side). For the INCA images, the *X* axis points roughly to the Sun, the *Z* axis is parallel to Saturn's spin vector, and *Y* completes the right-handed system. At the same time, RPWS recorded a typical narrowband radio emission lasting for about 7 h, from 0700 UT to 1400 UT.

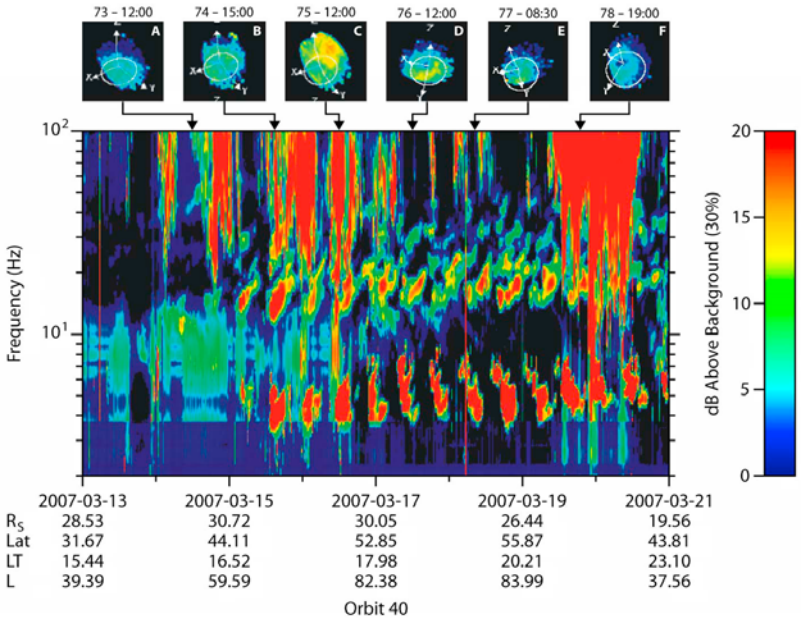

Figure 11. This plot combines an RPWS spectrogram and a sequence of six corresponding ENA images taken by MIMI/INCA and shows an example of a simultaneous onset of narrowband emissions and intensity increase of the hot rotating plasma. Cassini was in the Northern Hemisphere and was looking down toward Saturn. The white circle shows the orbit of Titan (20.2 R_s). The maximum intensity blob (yellow to red, at C) is more intense by a factor of ~10 compared to the lowest observable intensity (blue).

May 2007. In total, there are 30 events. The second and third columns give the start and stop time of each event. The fourth and fifth columns show the corresponding latitude and local time range of the spacecraft for each event. For the last two columns, we study whether there is an accompanying hot plasma cloud and if there were simultaneous onsets when those events occurred. Among the 30 events listed, no MIMI/INCA data are available for 7 of them, because during those events Cassini was on the nightside looking toward the dayside and INCA was shut down to protect the camera from incident sunlight. For the 23 events for which INCA data are available, there is only one event where no obvious intensified hot plasma cloud was observed. For this event, the camera was not pointed directly at Saturn the whole time, so this is similar to the situation of no data. For the time when the camera was pointed at Saturn, no hot plasma cloud was observed. This is probably because the ENA emission intensity falls off as $1/R^2$, so it would be difficult to identify the hot plasma cloud from 60 R_s away. In the following, we discuss the possible correlations between the narrowband emissions and the rotating hot plasma cloud.

[18] 1. Spatial correlation: *Carbary et al.* [2008] concluded that the radial distribution of ENA emissions maximizes near the orbit of Rhea (8.74 R_s) and *Krimigis et al.* [2007] shows that the inner edge of this plasma cloud could reach to the orbit of Dione (6.26 R_s). Our prediction of the 5 kHz narrowband component source location at L = 7.4 correlates well with the ENA emissions radial distribution. For 20–30 kHz or some higher-frequency bands, *Ye et al.* [2009] predicted their sources are located closer to the planet and to the equatorial plane compared to the 5 kHz component and the L shell is from 4 to 7. This predicted source location can still be covered by the plasma clouds but not with the strongest intensity, which probably can explain why the 20 to 30 kHz component is not as intense as the 5 kHz component.

[19] 2. Phase correlation: For different narrowband radio emission series, the phase position of the plasma cloud varies, but after looking through all the narrowband emission data and the ENA data, we see a strong trend for the plasma cloud to be moving through the dusk meridian and around to midnight (1800 – 2400 LT). As shown in Figure 10, when narrowband radio emissions occur, the major part of the plasma cloud is sweeping through the local evening sector. Within one event, the plasma cloud shows up at exactly the same phase at which the narrowband radio emissions are detected (auxiliary material Animation S1).[1] As we have seen from Figures 5 and 6, narrowband emissions tend to be observed with Cassini on the nightside of Saturn. The ENA emissions tend to be most intense on the nightside as well [*Krimigis et al.*, 2005].

[20] 3. Simultaneous onset: Figure 11 combines an RPWS spectrogram and the corresponding ENA images and shows an example of a nearly simultaneous onset between the narrowband radio emissions and the hot plasma cloud. Figure 11 (top) shows a sequence of six INCA images covering a 5 day interval. Before day 74 (15 March), when no narrowband emissions are observed, INCA does not see evidence of a rotating plasma cloud. The nearly simultaneous onset begins shortly after noon on day 74, as the plasma cloud starts to intensify, the narrowband emissions also intensify. Such comparison between these two phenomena can only be done when INCA as well as RPWS are observing, and the additional requirement for a certain spacecraft position results

[1] Auxiliary materials are available in the HTML. doi:10.1029/2009JA014847.

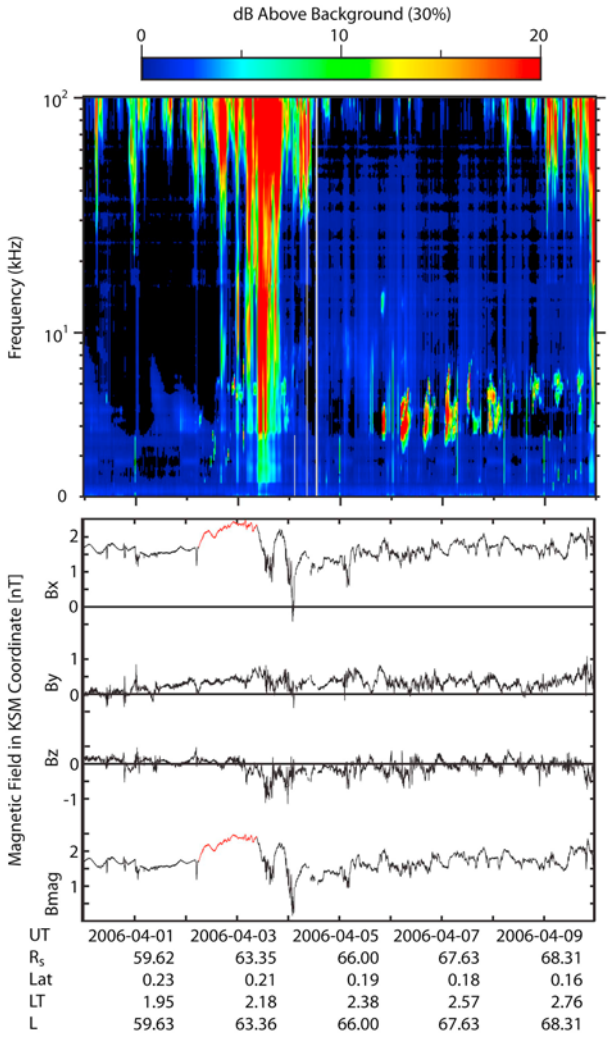

Figure 12. Comparison of radio observations by RPWS with magnetic field observations by MAG. The KSM coordinate system has Saturn at its origin, with the X axis directed toward the Sun; Z is defined such that Saturn's rotation and magnetic axes lie in the XZ plane (with $+Z$ pointing close to northward), and Y lying in Saturn's rotational and magnetic equatorial plane. The red curves in B_X and B_{MAG} highlight the enhancements by a factor of 2 in the magnetic field that are consistent with a compression of the magnetotail.

in a very limited number of events that can be compared. The "Simultaneous Onset" column of Table 1 records all these time intervals. Five narrowband emission events have a simultaneous onset with ENA emissions as shown in Figure 11. Some hot plasma clouds viewed from low latitudes do not have accompanying narrowband emissions, possibly because the dense plasma sheet prevents the radiation from propagating from the source region to the equatorial plane.

[21] *Mitchell et al.* [2009] demonstrated that, under some magnetospheric conditions, the hot plasma cloud rotating around Saturn is enhanced once per Saturn rotation. These recurrent enhancements coincide closely with bursts of SKR. It is suggested that the azimuthal asymmetry in the ring current pressure is the driver of the auroral field aligned current and consequently SKR. We propose that narrowband emissions are also associated with the rotating azimuthally asymmetric ring current as revealed by ENA images. *Carbary et al.* [2008] showed that the energetic oxygen atoms exhibit a very strong, repeatable periodicity of 10.8 h, which is close to the period of SKR as well as the narrowband radio emission, and this may suggest that the oxygen plasma cloud plays an important role in generating the narrowband radio emissions. As a clock (i.e., flashing light), the generation of narrowband emissions should be triggered when the hot plasma cloud rotates to a certain local time. So far, what process triggers the generation of narrowband emissions is still unclear. But to excite plasma waves, we need an anisotropy in the electron phase space distribution function. The anisotropy could be caused by the same electron precipitation process that produces aurora, which leaves behind an unstable loss cone distribution. Alternatively, a temperature anisotropy could be induced by a sudden change in magnetic field configuration such as the rapid dipolarization of the nightside magnetosphere after a reconnection. The second picture is consistent with the phase correlation between narrowband emissions and ENA emissions, where the rotating hot plasma cloud is mostly in the evening to midnight sector when narrowband emissions are observed.

[22] Comparison with MAG (Magnetometer) data shows that the narrowband radio emissions at Saturn are strongly correlated with a magnetic field compression in the magnetotail. With Cassini in the magnetotail for the week before and after the start time of the narrowband events (more than ten events), clear compressions of the magnetotail are detected by MAG, which are reflected by different signatures on the magnetic field plots. Figures 12 and 13 are two such plots. Figure 12 shows observations by RPWS and MAG for 10 days, from 31 March to 10 April 2006. Figure 12 (top) is the RPWS dynamic spectrum. Figure 12 (bottom) is the plot of the corresponding magnetic field, and from top to bottom, are the B_X, B_Y, B_Z components, and the magnitude B_{MAG} in the kronocentric solar magnetospheric (KSM) coordinate system [*Dougherty et al.*, 2005]. The red curves in B_X and B_{MAG} highlight the enhancements by a factor of 2 in the magnetic field that are consistent with a compression of the magnetotail. About 2 days after the compression, RPWS detected a series of 5 kHz narrowband radio emissions. Figure 13 covers an observation by MAG of parts of orbit 27 and 28, from day 231 to 246, 2006. Besides changes in the x and y components in the KSM system, Cassini was traveling southward in the $-z$ direction for the entire time. The plot shows the magnetic field in the KSM coordinate system while Cassini was in the magnetotail and recorded another compression of the tail by a factor of 4. The enhancements of B_x and B_{mag} in Figure 13 are not as obvious as those in Figure 12 because Cassini was hovering around the current sheet on this orbit, so that may have affected what MAG detected. The compression started on day 231, which is 19 August. Narrowband radio emissions started on 22 August, the third day that the tail is compressed. The red line of the B_{mag} marks the tracking of the background field. From day 232 to 238 there is an enhancement in the magnetic field strength that is driven by the B_x component, which means a compression of the tail. Initially, Cassini is in the northern lobe of the magnetotail, so B_x has a negative value as the magnetic field lines at Saturn start from the north pole and end in the south pole. The following positive values of B_x indicate that Cassini moved from

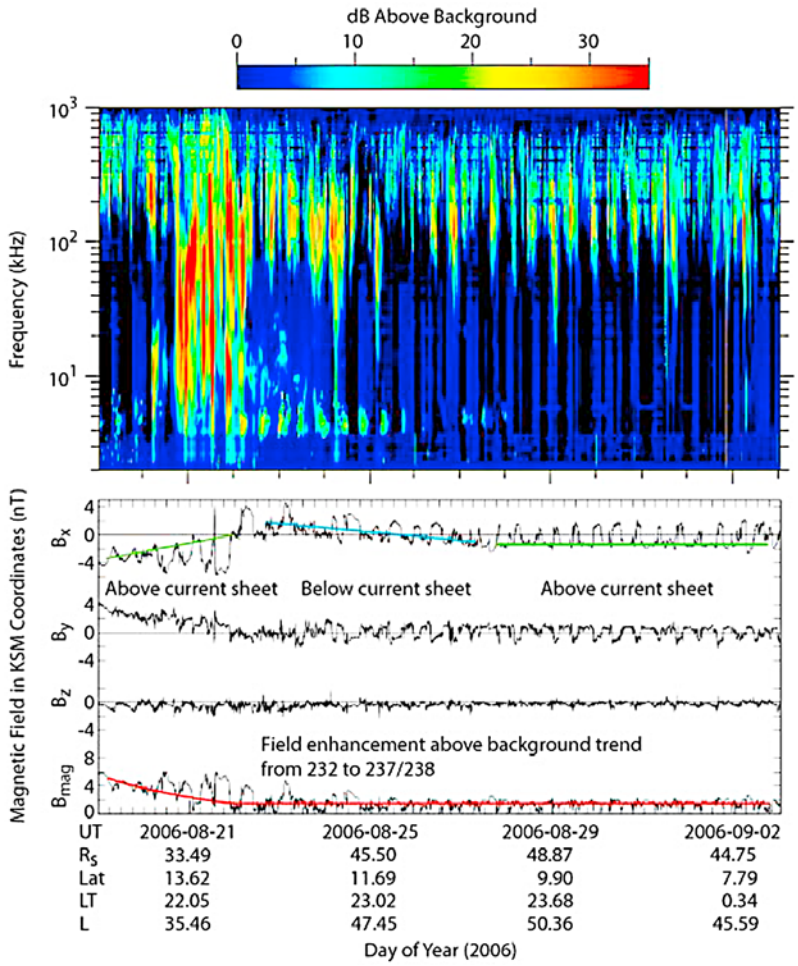

Figure 13. RPWS spectrogram and corresponding magnetic field observations in the KSM coordinate system during a magnetotail compression in August 2006. The KSM coordinate system has been defined in the caption of Figure 12.

the northern lobe to the southern lobe, and then gradually returned to the northern lobe, all while continuing to move southward. The only way that could happen is if the current sheet was pushed northward, and then relaxed and moved back south of Cassini. This kind of current sheet motion and the enhancement in the field can only be explained by a compression of the magnetotail. We believe that the frequency drift of the narrowband emission events to higher frequencies (see Figure 3) is due to the restoration of the magnetic field to its original state after the compression of the magnetotail. As the magnetic field moves back to its original state, the sources of narrowband emissions move toward the planet as well as to high latitudes so that the upper hybrid frequencies increase since the cyclotron frequencies or the magnetic field strength surrounding the source locations increase.

6. Discussion and Conclusions

[23] In this paper, we describe and analyze the narrowband radio emissions detected by the Cassini RPWS instrumentation from September 2005 to May 2007. The most intense narrowband emissions occur near 5 kHz with a 10.8 h modulation and a slow upward frequency drift of a few hundred Hz per day. Some emissions occur at higher frequencies, typically around 20–30 kHz with much lower intensity. The 20–30 kHz component does not show a periodic nature as clear as the 5 kHz component. The narrowband emissions are usually observed 1 or 2 days after an SKR intensity increase. Analysis based on 2 years of data shows that 5 kHz narrowband emissions tend to be observed in the evening sector, as well as at higher latitudes (>30 degrees), and that the detection of 20–30 kHz narrowband emissions has no local time preference while being confined to higher latitude (>40 degrees). Unlike the Jovian narrowband radio emission [*Kaiser and Desch*, 1980], which has a modulation like a rotating beacon, the modulation of the Saturnian narrowband radio emission is like a flashing light, similar to the SKR. Why Saturn's narrowband emissions have such a rotational modulation is poorly understood and needs further study.

[24] We briefly discussed the generation mechanism. At Earth and Jupiter, mode conversion from electrostatic upper hybrid waves has now been widely accepted to explain the generation of narrowband radio emissions. This mechanism is consistent with the observed polarization of the radio emissions, which indicates propagation in the L-O mode. Electrostatic waves are mode converted to electromagnetic waves near the upper hybrid frequency in the regions where sharp plasma density gradients exist. At Saturn, this region is

believed to be near the northern and southern boundaries of the plasma sheet. We also discussed a model for the source location for the 5 kHz emission band and worked out the corresponding L shell as L = 7.4. The rotating hot plasma clouds revealed by the MIMI/INCA instrument are recognized as a possible source for narrowband radio emissions. Since the modulation of the narrowband emissions is more like a flashing light rather than a rotating beacon, it could be that the rotating plasma cloud triggers the emissions when passing through some magnetic local time sector. This is similar for SKR, and as with the SKR the exact interaction process is still unclear.

[25] **Acknowledgments.** We thank S. M. Krimigis (PI of Cassini/MIMI) and M. K. Dougherty (PI of Cassini/MAG) for providing the Cassini MIMI/INCA data and the Cassini Magnetometer data. This work was supported by Jet Propulsion Laboratory contract 1279973 with the University of Iowa.

[26] Amitava Bhattacharjee thanks Philippe Louarn and another reviewer for their assistance in evaluating this paper.

References

Ashour-Abdalla, M., and C. F. Kennel (1978), Nonconvective and convective electron cyclotron harmonic instabilities, *J. Geophys. Res.*, *83*, 1531–1543, doi:10.1029/JA083iA04p01531.

Barbosa, D. D. (1982), Low-level VLF and LF radio emissions observed at Earth and Jupiter, *Rev. Geophys.*, *20*, 316–334, doi:10.1029/RG020i002p00316.

Carbary, J. F., D. G. Mitchell, P. Brandt, E. C. Roelof, and S. M. Krimigis (2008), Statistical morphology of ENA emissions at Saturn, *J. Geophys. Res.*, *113*, A05210, doi:10.1029/2007JA012873.

Cecconi, B., and P. Zarka (2005), Direction finding and antenna calibration through analytical inversion of radio measurements performed using a system of two or three electric dipole antennas on a three-axis stabilized spacecraft, *Radio Sci.*, *40*, RS3003, doi:10.1029/2004RS003070.

Dougherty, M. K., et al. (2005), Cassini Magnetometer observations during Saturn orbit insertion, *Science*, *307*, 1266–1270, doi:10.1126/science.1106098.

Farrell, W. M., W. S. Kurth, M. L. Kaiser, M. D. Desch, D. A. Gurnett, and P. Canu (2005), Narrowband Z-mode emissions interior to Saturn's plasma torus, *J. Geophys. Res.*, *110*, A10204, doi:10.1029/2005JA011102.

Fischer, G., S.-Y. Ye, D. A. Gurnett, W. S. Kurth, and Z. Wang (2008), The polarization of Saturn narrowband radio emissions, paper presented at European Geosciences Union Meeting, Vienna, Austria, April 13–18.

Gurnett, D. A. (1975), The Earth as a radio source: The nonthermal continuum, *J. Geophys. Res.*, *80*, 2751–2763, doi:10.1029/JA080i019p02751.

Gurnett, D. A., and A. Bhattacharjee (2005), *Introduction to Plasma Physics with Space and Laboratory Applications*, Cambridge Univ. Press, Cambridge, U. K.

Gurnett, D. A., and R. R. Shaw (1973), Electromagnetic radiation trapped in the magnetosphere above the plasma frequency, *J. Geophys. Res.*, *78*, 8136–8149, doi:10.1029/JA078i034p08136.

Gurnett, D. A., W. S. Kurth, and F. L. Scarf (1981), Narrowband electromagnetic emissions from Saturn's magnetosphere, *Nature*, *292*, 733–737, doi:10.1038/292733a0.

Gurnett, D. A., W. S. Kurth, and F. L. Scarf (1983), Narrowband electromagnetic emissions from Jupiter's magnetosphere, *Nature*, *302*, 385–388, doi:10.1038/302385a0.

Gurnett, D. A., et al. (2004), The Cassini radio and plasma wave investigation, Space Sci. *Rev.*, *114*, 395–463, doi:10.1007/s11214-004-1434-0.

Gurnett, D. A., A. M. Persoon, W. S. Kurth, J. B. Groene, T. F. Averkamp, M. K. Dougherty, and D. J. Southwood (2007), The variable rotational period of the inner region of Saturn's plasma disk, *Science*, *316*, 442–445, doi:10.1126/science.1138562.

Horne, R. B. (1989), Path-Integrated growth of electrostatic waves: The generation of terrestrial myriametrc radiation, *J. Geophys. Res.*, *94*, 8895–8909, doi:10.1029/JA094iA07p08895.

Horne, R. B. (1990), Narrow-band structure and amplitude of terrestrial myriametric radiation, *J. Geophys. Res.*, *95*, 3925–3932, doi:10.1029/JA095iA04p03925.

Hubbard, R. F., and T. J. Birmingham (1978), Electrostatic emissions between electron gyroharmonics in the outer magnetosphere, *J. Geophys. Res.*, *83*, 4837–4850, doi:10.1029/JA083iA10p04837.

Jones, D. (1976), Source of terrestrial nonthermal radiation, *Nature*, *260*, 686–689, doi:10.1038/260686a0.

Jones, D. (1983), Source of Saturn myriametric radiation, *Nature*, *306*, 453–456, doi:10.1038/306453a0.

Jones, D. (1988), Planetary radio emissions from low magnetic latitude: Observations and theories, in *Planetary Radio Emissions II*, edited by H. O. Rucker, S. J. Bauer, and B. M. Pedersen, pp. 255–293, Austrian Acad. of Sci. Press, Vienna.

Kaiser, M. L., and M. D. Desch (1980), Narrow-band Jovian kilometric radiation: A new radio component, *Geophys. Res. Lett.*, *7*, 389–392, doi:10.1029/GL007i005p00389.

Krimigis, S. M., et al. (2005), Dynamics of Saturn's magnetosphere from MIMI during Cassini's orbital insertion, *Science*, *307*, 1270–1273, doi:10.1126/science.1105978.

Krimigis, S. M., N. Sergis, D. G. Mitchell, D. C. Hamilton, and N. Krupp (2007), A dynamic, rotating ring current around Saturn, *Nature*, *450*, 1050–1053, doi:10.1038/nature06425.

Kurth, W. S., D. A. Gurnett, and R. R. Anderson (1981), Escaping nonthermal continuum radiation, *J. Geophys. Res.*, *86*, 5519–5531, doi:10.1029/JA086iA07p05519.

Kurth, W. S., T. F. Averkamp, D. A. Gurnett, J. B. Groene, and A. Lecacheux (2008), An update to a Saturnian longitude system based on kilometric radio emissions, *J. Geophys. Res.*, *113*, A05222, doi:10.1029/2007JA012861.

Lamy, L., P. Zarka, B. Cecconi, R. Prangé, W. S. Kurth, and D. A. Gurnett (2008), Saturn kilometric radiation: Average and statistical properties, *J. Geophys. Res.*, *113*, A07201, doi:10.1029/2007JA012900.

Louarn, P., et al. (2007), Observation of similar radio signatures at Saturn and Jupiter: Implications for the magnetospheric dynamics, *Geophys. Res. Lett.*, *34*, L20113, doi:10.1029/2007GL030368.

Melrose, D. B. (1981), A theory for the nonthermal radio continua in the terrestrial and Jovian magnetosphere, *J. Geophys. Res.*, *86*, 30–36, doi:10.1029/JA086iA01p00030.

Menietti, J. D., S.-Y. Ye, P. H. Yoon, O. Santolik, A. M. Rymer, D. A. Gurnett, and A. J. Coates (2009), Analysis of narrowband emission observed in the Saturn magnetosphere, *J. Geophys. Res.*, *114*, A06206, doi:10.1029/2008JA013982.

Mitchell, D. G., et al. (2009), Recurrent energization of a plasma in the midnight-to-dawn quadrant of Saturn's magnetosphere, and its relationship to auroral UV and radio emissions, *Planet. Space Sci.*, *57*, 1732–1742, doi:10.1016/j.pss.2009.04.002.

Persoon, A. M., D. A. Gurnett, W. S. Kurth, and J. B. Groene (2006), A simple scale height model of the electron density in Saturn's plasma disk, *Geophys. Res. Lett.*, *33*, L18106, doi:10.1029/2006GL027090.

Rönnmark, K. (1983), Emissions of myriametric radiation by coalescence of upper hybrid waves with low frequency waves, *Ann. Geophys.*, *1*, 187–192.

Rönnmark, K. (1989), Myriametric radiation and the efficiency of linear mode conversion, *Geophys. Res. Lett.*, *16*, 731–734, doi:10.1029/GL016i007p00731.

Rönnmark, K. (1992), Conversion of upper hybrid waves into magnetospheric radiation, in *Planetary Radio Emissions III*, edited by H. O. Rucker, S. J. Bauer, and M. L. Kaiser, pp. 405–417, Austrian Acad. of Sci, Vienna.

Rönnmark, K., H. Borg, P. J. Christiansen, M. P. Gough, and D. Jones (1978), Banded electron-cyclotron harmonic instability—A first comparison between theory and experiment, *Space Sci. Rev.*, *22*, 401–417, doi:10.1007/BF00210876.

Warwick, J. W., et al. (1981), Planetary radio astronomy observations from Voyager 1 near Saturn, *Science*, *212*, 239–243, doi:10.1126/science.212.4491.239.

Ye, S.-Y., et al. (2009), Source locations of narrowband radio emissions detected at Saturn, *J. Geophys. Res.*, *114*, A06219, doi:10.1029/2008JA013855.

Zarka, P. (1998), Auroral radio emissions at the outer planets: Observations and theories, *J. Geophys. Res.*, *103*, 20,159–20,194, doi:10.1029/98JE01323.

Zarka, P., L. Lamy, B. Cecconi, R. Prange, and H. O. Rucker (2007), Modulation of Saturn's radio clock by solar wind speed, *Nature*, *450*, 265–267, doi:10.1038/nature06237.

G. Fischer, D. A. Gurnett, W. S. Kurth, J. S. Leisner, Z. Wang, and S.-Y. Ye, Department of Physics and Astronomy, University of Iowa, 713 Van Allen Hall, Iowa City, IA 52242, USA. (zhenzhen-wang@uiowa.edu)

D. G. Mitchell, Johns Hopkins University Applied Physics Laboratory, 11100 Johns Hopkins Rd., Laurel, MD 20723, USA.

C. T. Russell, Institute of Geophysics and Planetary Physics, University of California, 603 Charles Young Dr. E., 3845 Slichter Hall, Los Angeles, CA 90095, USA.